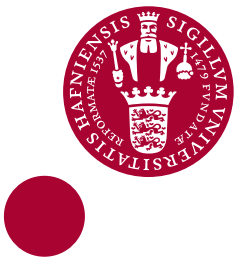

PTIP chromatin regulator controls development and activation of B cell subsets to license humoral immunity in mice

Su, Dan; Vanhee, Stijn; Soria, Rebeca; Gyllenbäck, Elin Jaensson; Starnes, Linda M; Højfeldt, Martina Kubec; Pedersen, Gabriel K; Yuan, Joan; Daniel, Jeremy A

Published in:
Proceedings of the National Academy of Sciences of the United States of America

DOI:
10.1073/pnas.1707938114

Publication date:
2017

Document version
Publisher's PDF, also known as Version of record

PTIP chromatin regulator controls development and activation of B cell subsets to license humoral immunity in mice

Dan Su[a], Stijn Vanhee[b], Rebeca Soria[a], Elin Jaensson Gyllenbäck[b], Linda M. Starnes[a], Martina Kubec Højfeldt[a], Gabriel K. Pedersen[c], Joan Yuan[b,1], and Jeremy A. Daniel[a,1]

[a]Chromatin Structure and Function Group, The Novo Nordisk Foundation Center for Protein Research, Faculty of Health and Medical Sciences, University of Copenhagen, Copenhagen, Denmark 2200; [b]Developmental Immunology Group, Division of Molecular Hematology, Lund Stem Cell Center, Faculty of Medicine, Lund University, Lund, Sweden 22184; and [c]Department of Infectious Disease Immunology, Statens Serum Institute, Copenhagen, Denmark 2300

Edited by Klaus Rajewsky, Max Delbrück Center for Molecular Medicine, Berlin, Germany, and approved September 20, 2017 (received for review May 13, 2017)

B cell receptor signaling and downstream NF-κB activity are crucial for the maturation and functionality of all major B cell subsets, yet the molecular players in these signaling events are not fully understood. Here we use several genetically modified mouse models to demonstrate that expression of the multifunctional BRCT (BRCA1 C-terminal) domain-containing PTIP (Pax transactivation domain-interacting protein) chromatin regulator is controlled by B cell activation and potentiates steady-state and postimmune antibody production in vivo. By examining the effects of PTIP deficiency in mice at various ages during ontogeny, we demonstrate that PTIP promotes bone marrow B cell development as well as the neonatal establishment and subsequent long-term maintenance of self-reactive B-1 B cells. Furthermore, we find that PTIP is required for B cell receptor- and T:B interaction-induced proliferation, differentiation of follicular B cells during germinal center formation, and normal signaling through the classical NF-κB pathway. Together with the previously identified role for PTIP in promoting sterile transcription at the *Igh* locus, the present results establish PTIP as a licensing factor for humoral immunity that acts at several junctures of B lineage maturation and effector cell differentiation by controlling B cell activation.

antibody | B cell biology | B-1 | IgM | immunodeficiency

The full spectrum of vertebrate humoral antibody immunity is made up of natural antibodies and postimmune antigen-specific antibodies (1). Natural antibodies are produced by innate-like B-1 cells enriched for reactivities to carbohydrate moieties found on common microbial pathogens as well as self-glycolipids and play an established role in immune surveillance and the clearance of cellular debris (2). Together with marginal zone (MZ) B cells, B-1 cells also mount rapid thymus-independent (TI) antibody responses against blood-borne pathogens and provide an important first line of defense during early stages of infection (3, 4). The far more prevalent follicular (FO) B-2 B cell subset, on the contrary, undergoes T-dependent (TD) affinity maturation and antibody class-switch recombination (CSR) in germinal centers (GCs) of secondary lymphoid organs to provide high-affinity IgG responses during the later stages of infection as well as immunological memory. Together, the different B cell subsets perform nonredundant functions to provide optimal host defense.

The PTIP protein is a ubiquitously expressed, nuclear-localized chromatin regulator containing six BRCT (BRCA1 C-terminal) domains. It has been described as an adaptor protein and is implicated in gene regulation, DNA replication, and DNA repair (5). Even though PTIP associates with the MLL3/MLL4 methyltransferase complex, it also has the capacity to function in gene expression independently from this complex (6) and in DNA repair with the 53BP1 protein (7). In B cells, PTIP is required for sterile transcription of switch regions at the Ig heavy-chain (*Igh*) locus and subsequent IgH CSR to multiple IgG isotypes in a manner independent from MLL3/MLL4 (6, 8, 9). Here we use mouse genetics to demonstrate that PTIP additionally establishes steady-state and postimmune IgM and IgG antibody production in vivo by regulating the development, activation, and survival of B cell subsets, at least in part, via the classical NF-κB signaling pathway.

Results

PTIP Is Required for Antibody Production in Vivo. PTIP is known to facilitate IgH class-switching in stimulated B cells ex vivo (6, 8). To begin to determine the role of PTIP in antibody responses in vivo, we immunized $CD19^{cre/+}PTIP^{flox/flox}$ (referred to here as $PTIP^{-/-}$) mice and assayed antigen-specific antibody levels from serum over a 3-wk period. We used TNP-LPS as a TI type 1 antigen, TNP-Ficoll as a TI type 2 antigen, and TNP-KLH as a TD antigen. Serum from $PTIP^{-/-}$ mice harbored a near-complete block in the levels of TNP-specific IgG3 after immunization compared with $CD19^{cre/+}PTIP^{+/+}$ controls (referred to as WT) at 7 d postimmunization (Fig. 1 *A*–*C*, *Right*), in line with previous ex vivo findings (6, 8). IgG1 and IgG2b responses were similarly altered in $PTIP^{-/-}$ mice (Fig. S1 *A*–*C*).

Significance

To provide optimal host defense, the full spectrum of antibody-based immunity requires natural antibodies and immunization-induced antigen-specific antibodies. Here we show that the PTIP (Pax transactivation domain-interacting protein) chromatin regulator is induced by B cell activation to potentiate the establishment of steady-state and postimmune serum antibody levels. It does so by promoting activation-associated proliferation and differentiation of all the major B cell subsets, at least in part, through regulating the NF-κB pathway. With the genetic basis still unknown for a majority of patients with common variable immunodeficiency, further work investigating how PTIP controls cell signaling may generate valuable new insight for human health and disease.

Author contributions: J.Y. and J.A.D. designed research; D.S., S.V., R.S., E.J.G., and M.K.H. performed research; D.S., S.V., and L.M.S. contributed new reagents/analytic tools; D.S., S.V., R.S., E.J.G., G.K.P., J.Y., and J.A.D. analyzed data; J.Y. and J.A.D. wrote the paper; and G.K.P. contributed NF-κB expertise.

The authors declare no conflict of interest.

This article is a PNAS Direct Submission.

Data deposition: The data reported in this paper have been deposited in the Gene Expression Omnibus (GEO) database, https://www.ncbi.nlm.nih.gov/geo (accession no. GSE98402).

[1]To whom correspondence may be addressed. Email: joan.yuan@med.lu.se or jeremy.daniel@cpr.ku.dk.

This article contains supporting information online at www.pnas.org/lookup/suppl/doi:10.1073/pnas.1707938114/-/DCSupplemental.

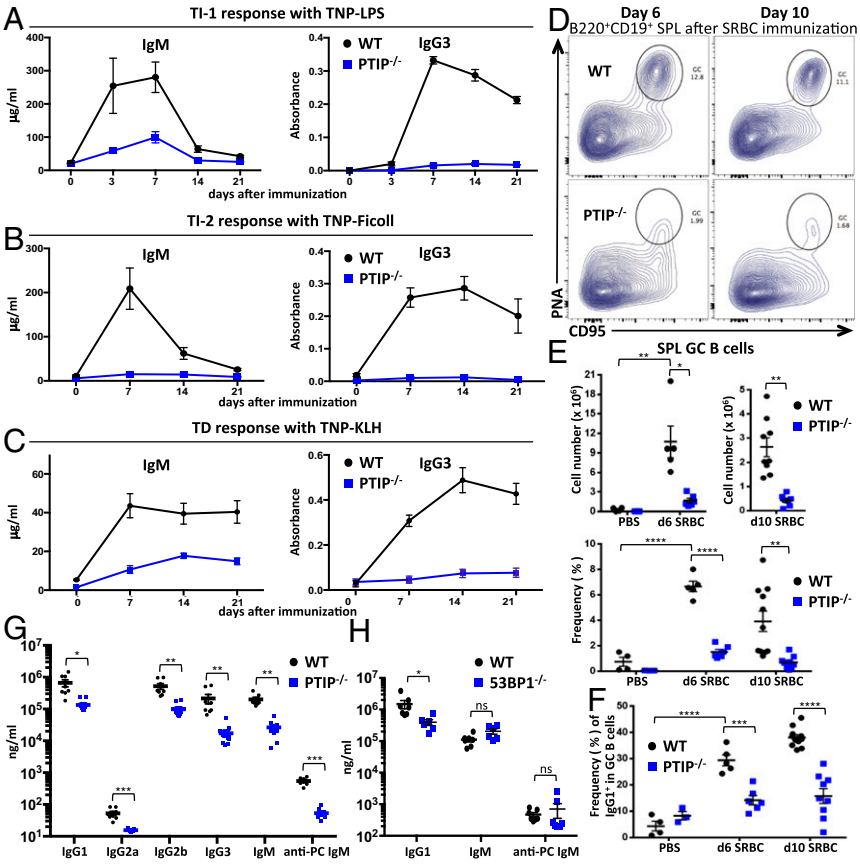

Fig. 1. PTIP is required for steady-state and antigen-induced antibody production in vivo. Mice were immunized with (*A*) TNP-LPS, (*B*) TNP-Ficoll, or (*C*) TNP-KLH, and anti-TNP-specific IgM or IgG3 serum levels were measured by ELISA at the indicated days before and after immunization. Data are from four mice of each genotype in *A*, four mice in *B*, and seven mice in *C*, and are plotted as Ig concentration or the absorbance for the serum dilution that gave half optical density (mean ± SEM). Experiments were repeated at least two times. *P* values at 7 d after immunization are as follows: (*A*) IgM, $*P = 0.03$; IgG3, $****P < 0.0001$; (*B*) IgM, $*P = 0.02$; IgG3, $***P = 0.0003$; (*C*) IgM, $***P = 0.001$; IgG3, $****P < 0.0001$. (*D*) Flow cytometric analysis of GC B cells in the spleen at the indicated days after immunization with SRBCs. (*E*) GC B cell numbers (*Top*) and frequencies (*Bottom*) from spleens (as in *D*) of at least three mice with PBS, five mice at 6 d, and nine mice at 10 d per genotype postimmunization. Data are presented as mean ± SEM. (*Top*) Day 6, $*P = 0.02$; day 10, $**P = 0.003$; PBS vs. day 6 in WT, $**P = 0.001$. (*Bottom*) Day 6, $****P < 0.0001$; day 10, $**P = 0.002$; PBS vs. day 6 in WT, $****P < 0.0001$. (*F*) Flow cytometric analyses of IgG1$^+$ frequencies among GC B cells as in *D*. Data are presented as mean ± SEM. Day 6, $***P = 0.0005$; day 10, $****P < 0.0001$; PBS vs. day 6 in WT, $****P < 0.0001$. (*G*) ELISA analysis of total Ig levels from sera of unimmunized mice. Data are from at least six mice of each genotype and are presented as mean ± SEM. IgG1, $*P = 0.015$; IgG2a, $***P = 0.001$; IgG2b, $**P = 0.005$; IgG3, $**P = 0.004$; IgM, $**P = 0.002$; anti-PC IgM, $***P = 0.0006$. (*H*) ELISA analysis of total Ig levels from sera of unimmunized mice. Data are from at least six mice of each genotype and are presented as mean ± SEM. IgG1, $*P = 0.046$; others not significant (ns). Statistics were generated by using a two-tailed unpaired *t* test with Welch's correction.

Interestingly, *PTIP*$^{-/-}$ mice showed impaired levels of TNP-specific IgM across the three different immunization schemes, ranging from 2.8- to 14-fold decreases at 7 d postimmunization, suggesting a physiological role beyond regulation of CSR (Fig. 1 *A*–*C*, *Left*). We conclude that PTIP promotes antigen-specific IgM and IgG responses in vivo, despite being largely dispensable for the development of most splenic B cells (8) (Fig. S1*D*).

In view of the profound impairments in antibody responses to TI and TD antigens in PTIP-deficient mice, we examined GC formation in these mice. Mice were immunized with the TD antigen sheep red blood cells (SRBCs) and GC B cells were assayed from spleens. At 6 and 10 d postimmunization, *PTIP*$^{-/-}$ mice displayed severely impaired frequencies and numbers of GC (CD19$^+$B220$^+$PNA$^+$CD95$^+$) B cells compared with control mice (Fig. 1 *D* and *E*). Consistent with IgG1 class-switching defects associated with PTIP deficiency (6, 8) (Fig. S1 *A*–*C*), IgG1$^+$ frequencies were also impaired among GC B cells in SRBC-immunized *PTIP*$^{-/-}$ mice compared with controls (Fig. 1*F* and Fig. S1*E*). We conclude that PTIP promotes TD GC B cell differentiation after immunization in vivo.

To determine antibody levels at steady state, we analyzed serum from unimmunized animals. We found that *PTIP*$^{-/-}$ mice displayed a 7.6-fold decrease in serum IgM levels in addition to severely reduced IgG1, IgG2a, IgG2b, and IgG3 levels (Fig. 1*G*). At steady state, IgM antibodies are highly enriched for specificities against carbohydrate moieties such as phosphorylcholine (PC) and serve an important function in immune surveillance and the removal of cellular debris (2). To determine whether the decrease in steady-state serum IgM levels from *PTIP*$^{-/-}$ mice was linked to a deficiency in such protective natural antibodies, we measured PC-specific IgM titers and observed a 10-fold decrease (Fig. 1*G*). Thus, PTIP critically potentiates steady-state and postimmune levels of IgM and IgG antibodies in vivo.

PTIP harbors DNA repair functions that are, at least in part, mediated by its physical association with 53BP1 (7); however, consistent with other reports (10, 11), we found decreased IgG1 but normal total IgM in the serum of *53BP1*$^{-/-}$ mice (Fig. 1*H*). In addition, PC-specific IgM levels from *53BP1*$^{-/-}$ mice were indistinguishable from those from controls (Fig. 1*H*). Furthermore, even though antigen-specific IgG3 levels were severely impaired upon challenging *53BP1*$^{-/-}$ mice with the TI type 2 TNP-Ficoll antigen, we found antigen-specific IgM to be indistinguishable vs. controls (Fig. S1*F*). These results suggest that PTIP promotes natural and antigen-induced IgM levels independently from its association with 53BP1 and its involvement in DNA repair.

PTIP Deficiency Causes a Partial Block in B Cell Development. To begin to investigate the underlying cause for such profound immunodeficiency, we analyzed the B cell compartments in unperturbed *PTIP*$^{-/-}$ mice. Bone marrow from *PTIP*$^{-/-}$ and control mice was first analyzed to ascertain whether loss of PTIP affects B cell development. Although no differences were observed in pro-B (CD93$^+$B220$^+$CD19$^+$IgM$^-$CD43$^+$CD24^{med}) cells, numbers of small pre-B (CD93$^+$B220$^+$CD19$^+$IgM$^-$CD43$^-$CD24$^+$) cells were decreased 2.2-fold in *PTIP*$^{-/-}$ bone marrow compared with controls, along with a subtle 1.4-fold decrease in immature (CD93$^+$B220$^+$CD19$^+$IgM$^+$CD24$^+$) B cells (Fig. 2 *A* and *B*). Numbers of large pre-B (CD93$^+$B220$^+$CD19$^+$IgM$^-$CD43$^+$CD24^{hi}) cells and mature (CD93$^-$B220$^+$CD19$^+$IgM$^+$CD24$^-$) B cells in the bone marrow were concomitantly increased 1.9-fold and 1.5-fold, respectively, comparable to controls (Fig. 2 *A* and *B*). We conclude that loss of PTIP leads to a mild B cell development defect marked by an inefficient transition of large cycling

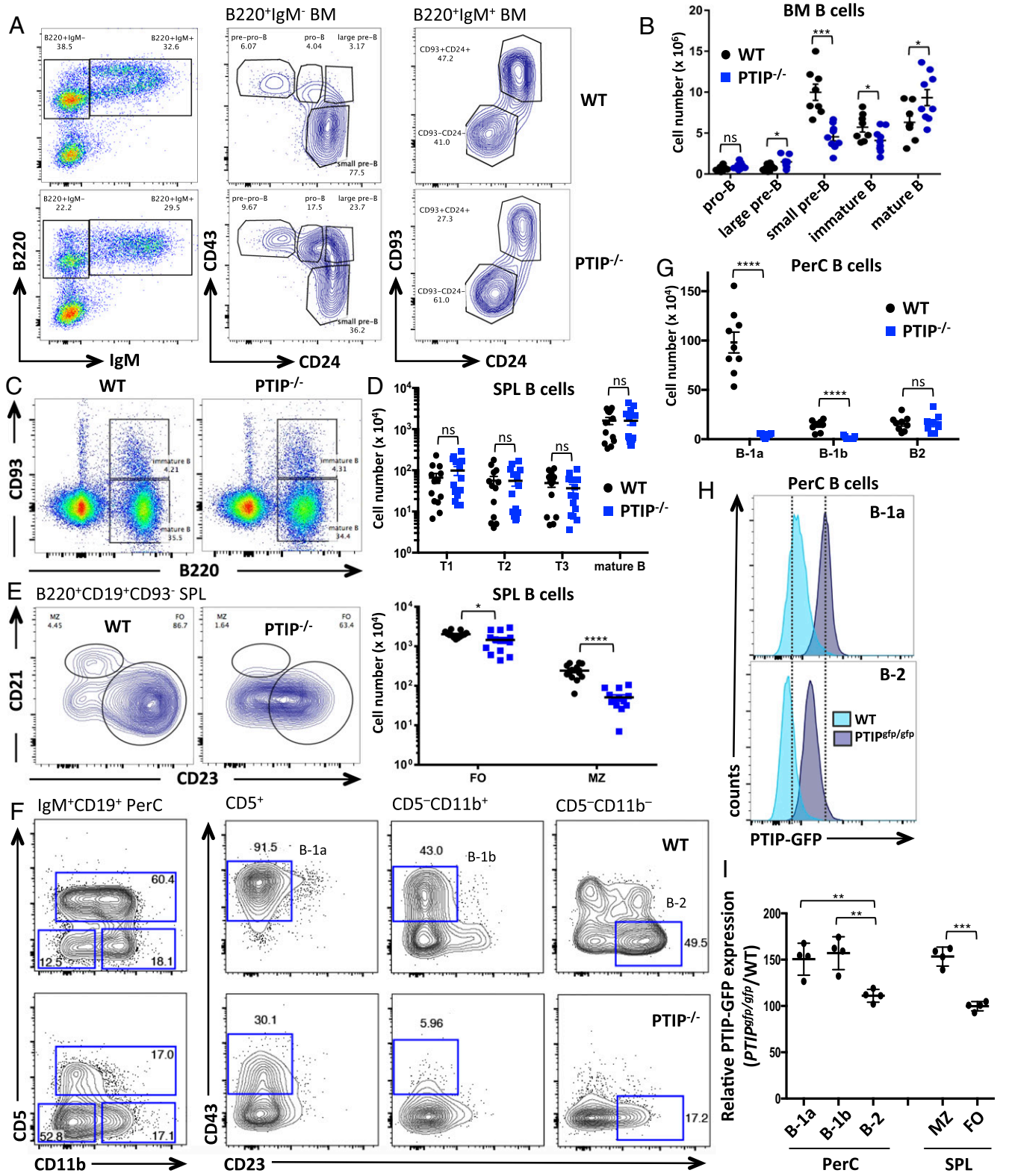

Fig. 2. PTIP deficiency causes a partial block in B cell development and impairs establishment of innate-like B cell subsets. (*A*) Flow cytometric analysis of bone marrow cells from adult mice. (*B*) Numbers of developing B cells from bone marrow of at least eight mice per genotype. Data are presented as mean ± SEM. Large pre-B, $*P = 0.02$; small pre-B, $***P = 0.0006$; immature B, $*P = 0.05$; mature B, $*P = 0.03$; pro-B, $P = 0.08$ [not significant (ns)]. (*C–E*) Flow cytometric analyses of splenic B cells from adult mice. (*D*) B cell numbers from spleens as in *C* and *E* from at least 13 mice. Data are presented as mean ± SEM. (*Top*) $P > 0.3$ for all comparisons, which is not significant (ns). (*Bottom*) FO, $*P = 0.028$; MZ, $****P < 0.0001$. (*F*) Flow cytometric analyses of peritoneal cavity B cells from adult mice. (*G*) B cell numbers from peritoneal cavities as in *F* from at least nine mice of each genotype. Data are presented as mean ± SEM. B-1a and B-1b, $****P < 0.0001$; B-2, $P = 0.9$, which is not significant (ns). (*H*) Flow cytometric analysis of PTIP-GFP expression in freshly isolated peritoneal cavity B cells. (*I*) Mean PTIP-GFP expression intensities from B cells as in *H* relative to WT controls from four mice. PerC, B-2 vs. B-1b, $**P = 0.009$; B-2 vs. B-1a, $**P = 0.01$; SPL, FO vs. MZ, $***P = 0.0005$. Statistics were performed by using a two-tailed unpaired *t* test with Welch's correction.

pre-B cells to small quiescent pre-B cells at a developmental time when Ig light-chain rearrangement is initiated in response to pre-B cell receptor (BCR) signaling.

PTIP Deficiency Impairs Establishment of Innate-Like B Cells. Spleens from *PTIP*$^{-/-}$ mice showed similar frequencies and numbers of transitional (CD93^{+}B220^{+}) and mature (CD93^{-}B220^{+}) B cells vs. control animals (Fig. 2 *C* and *D*), yet displayed a subtle 1.4-fold decrease in FO B cells (Fig. 2 *D* and *E*). In contrast, we observed a 4.7-fold decrease in the number of MZ B cells from *PTIP*$^{-/-}$ mice (Fig. 2 *D* and *E* and Fig. S2 *A*–*C*). This observation is intriguing, as MZ B cells contribute to TI IgM production (3) and share with B-1 B cells a stronger dependency on BCR-mediated signals for maturation and maintenance (3, 12, 13).

B-1 B cells largely reside in the peritoneal cavity and, in mice, are divided into the CD5^{+} B-1a subset, which preferentially mature during fetal and neonatal life, and the continuously replenished CD5^{-} B-1b subset. To determine whether the defect in natural IgM production in *PTIP*$^{-/-}$ mice might be explained by PTIP regulation of B-1 B cells, we analyzed peritoneal cavity cells from *PTIP*$^{-/-}$ and control mice by FACS. Among CD19^{+}IgM^{+} peritoneal cavity B cells, we observed severe reductions in the frequencies and numbers of B-1a and B-1b cells (Fig. 2 *F* and *G* and Fig. S2 *D* and *E*). Specifically, B-1a (CD19^{+}IgM^{+}CD5^{+} CD43^{+}CD23^{-}) cells were nearly absent and B-1b (CD19^{+}IgM^{+} CD5^{-}CD43^{+}CD11b^{+}CD23^{-}) cell numbers were decreased by 9.6-fold compared with control mice (Fig. 2*G*). In stark contrast, the numbers of conventional B (CD19^{+}IgM^{+}CD5^{-}CD43^{-} CD11b^{-}CD23^{+}) cells in the peritoneal cavity were indistinguishable vs. control mice (Fig. 2*G*). A similar decrease in B-1a cell numbers was observed in the spleen (Fig. S2 *A* and *F*). Residual *PTIP*$^{-/-}$ B-1a and B-1b cells exhibited alterations in their surface phenotype, including lower expression levels of CD43 and CD11b (Fig. 2*F*); moreover, surface expression of B220 (Fig. 2 *A* and *C* and Fig. S2*G*) and CD23 (Fig. 2 *E* and *F* and Fig. S2*B*) were lower on conventional B cells from *PTIP*$^{-/-}$ mice compared with controls. We conclude that PTIP promotes the generation and/or maintenance of innate-like B-1a and B-1b cells in unperturbed mice. Our observation of the concomitant decrease in B-1 and MZ B cell populations in *PTIP*$^{-/-}$ mice likely explains the observed impairment in steady-state as well as antigen-induced IgM production (Fig. 1).

To better understand the requirement for PTIP protein in various B cell subsets, we measured PTIP expression at the single-cell level by using a previously described knock-in mouse model that expresses GFP-tagged PTIP under the control of its endogenous regulatory elements (*PTIP*$^{gfp/gfp}$) (6). Interestingly, PTIP-GFP protein levels were higher in the B-1a, B-1b, and MZ B cell populations compared with conventional B-2 cells (Fig. 2 *H* and *I*). Together with the GC defects, these results from innate-like B cells are consistent with a functional requirement for PTIP in cells that have a strong dependency on BCR-mediated signals for maturation and maintenance.

PTIP Is Required for Neonatal B Cell Maturation. With B cell development in the bone marrow only being mildly reduced, possibly leading to a slower establishment of mature conventional B cell pools, the profound loss of B-1 cells and natural IgM in mice lacking PTIP remained curious. To better understand the reason for such immunodeficiency, we further investigated B-1a cell maturation in greater detail. Shortly after birth, rapid accumulation of B-1a cells in the peritoneal cavity (Fig. 3*A*) coincides with the increase in total and PC-specific serum IgM levels, as seen in 3-wk-old WT mice (Fig. 3 *B* and *C*). Strikingly, only a negligible increase in B-1a cell numbers are found in PTIP$^{-/-}$ peritoneal cavities throughout ontogeny, and natural antibody titers remain flat-lined (Fig. 3 *A*–*C* and Fig. S3*A*).

B-1a cells are not efficiently generated in adult life and sustain their peripheral presence through bone marrow-independent self-maintenance (14). To assess if a maturation defect could contribute to the observed decrease in B-1a cell representation in PTIP-deficient mice, we analyzed transitional B cells from spleens of neonatal mice known to efficiently give rise to B-1a B cells (15). Compared with controls, spleens from 1-d-old neonatal *PTIP*$^{-/-}$ mice showed decreased frequencies of transitional (CD93^{+}B220^{+}) B cells, including lower cell numbers of the three distinct transitional stages: T1 (CD93^{+}B220^{+}IgM^{+}CD23^{-}), T2 (CD93^{+}B220^{+}IgM^{+}CD23^{+}), and T3 (CD93^{+}B220^{+}IgM^{lo}CD23^{-}; Fig. 3 *D* and *E*). Similar results were obtained for mature (CD93^{-}B220^{+}) B cells, and results were also similar at 2 d of age (Fig. 3 *D*–*F*). Remarkably, by 2 wk of age and later in adult mice as described earlier (Fig. 2 *C* and *D*), these splenic B cell maturation defects were no longer apparent (Fig. 3 *D*–*F*). A developmentally restricted neonatal CD5^{+} transitional B cell subset (CD19^{+}CD93^{+}B220^{lo}IgM^{+}CD5^{+}) was recently identified that predominantly gives rise to B-1a cells (16). We readily detected the transient developmental wave of such CD5^{+} transitional B cells in 2-d- to 2-wk-old control mice; however, consistent with a defect in B-1a cell development, the percentage and absolute number of CD5^{+} transitional B cells showed a marked decrease in the absence of PTIP (Fig. 3 *G* and *H*). Moreover, *PTIP*$^{gfp/gfp}$ mice showed higher PTIP protein levels in transitional B cells from 3-d-old mice compared with mice at 5 or 12 wk of age (Fig. 3*I*), coinciding with the peak of B-1a cell output during ontogeny. These results collectively demonstrate a reliance on high PTIP expression during neonatal B lymphopoiesis, consistent with a requirement for PTIP for the output of B-1a cells and natural IgM levels.

PTIP-Deficient B-1a Cells Are Unable to Maintain Long-Term Survival of Self-Reactive Clones. B-1a cells are enriched for self-reactive specificities and rely mainly on self-antigen driven survival to maintain their peripheral population through life (12). The most common BCR specificity among B-1a cells is directed toward the self-glycolipid phosphatidylcholine (PtC) (17, 18) exposed on the surface of damaged cells. In light of the observed defects in neonatal B-1a cell development, we sought to understand whether the failure of B-1a cells to accumulate and establish a sizable population in PTIP-deficient mice is a consequence of an inability to produce a self-reactive BCR repertoire. To this end, we performed high-throughput *Igh-μ* repertoire analysis by (variable, diversity, joining) deep sequencing (VDJ-Seq) of the residual peritoneal cavity B-1a cell populations in 5- and 8-wk-old *PTIP*$^{-/-}$ mice (as shown in Fig. 2*F* and Fig. S3*A*). Upon extraction of the identities and frequencies of CDR3 clonotypes, we found the B-1a repertoire of 5-wk-old *PTIP*$^{-/-}$ mice to harbor comparable frequencies of PtC-reactive CDR3s vs. age-matched controls (Fig. 4 *A* and *B* and Fig. S3*B*). This result demonstrates that bona fide B-1a specificities can be generated in the absence of PTIP. Strikingly, the representation of this specificity is markedly decreased in 8-wk-old *PTIP*$^{-/-}$ mice, evident by a trend toward decreased usage of the VH12 segment known to encode the PtC specificity and an increased usage of VH4 (Fig. 4 *A*–*C*). Thus, although PTIP-deficient mice can successfully generate a small number of B-1a cells with the appropriate self-reactive BCR specificities, these clones fail to be maintained through self-antigen driven positive selection. Thus, the apparent lack of B-1a cells in adult *PTIP*$^{-/-}$ mice may be a compound effect from defects in B-1a cell maturation (Fig. 3) and peripheral maintenance.

To establish a direct role of PTIP in mature B-1a cell survival and maintenance in vivo without the influence of bone marrow influx, we FACS sorted *PTIP*$^{-/-}$ and control B-1a cells from 5-wk-old mice and transplanted equal numbers intraperitoneally into *RAG1*$^{-/-}$ recipient mice. Two weeks after transplantation, markedly fewer B cells remained in recipients of *PTIP*$^{-/-}$ cells compared with controls (Fig. 4*D*). This survival defect could be recapitulated upon in vitro culturing in media, in which *PTIP*$^{-/-}$

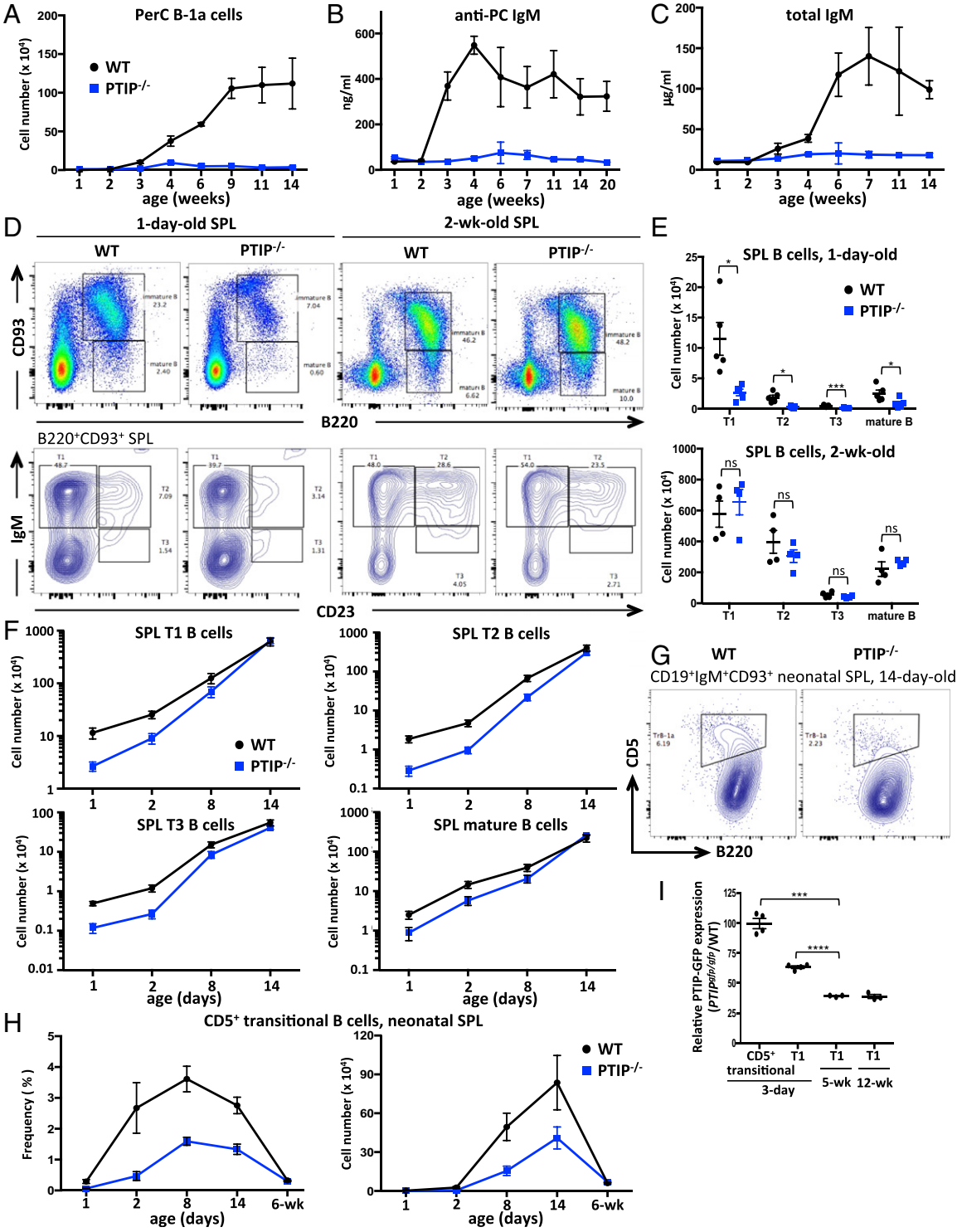

Fig. 3. PTIP is required for neonatal B cell maturation and the establishment of serum natural IgM levels. (*A*) B-1a cell numbers at the indicated age (in weeks) after birth. Data are from at least three mice for each age and genotype and are represented as mean ± SEM. (*B* and *C*) ELISA analysis of anti-PC IgM (*B*) and total IgM (*C*) levels from sera of unimmunized mice at the indicated age (in weeks) after birth. Data are from at least three mice for each age and genotype and are represented as mean ± SEM. At 3 wk, $^{**}P = 0.008$ for *A* and $^{**}P = 0.01$ for *B*. At 4 wk, $^{**}P = 0.009$ for *C*. (*D*–*F*) Flow cytometric analyses and cell numbers of splenic B cells at the indicated ages with at least four mice of each genotype per age. Data are presented as mean ± SEM. (*E*, *Top*) For 1 d old, T1 ($^{*}P = 0.029$), T2 ($^{*}P = 0.012$), T3 ($^{***}P = 0.002$), and mature B cells ($^{*}P = 0.04$); (*E*, *Bottom*) for 2 wk old, $P > 0.3$ for all comparisons, which is not significant (ns). (*F*) For 2 d old, T1 ($^{*}P = 0.02$), T2 ($^{*}P = 0.02$), T3 ($^{*}P = 0.025$), and mature B cells ($^{*}P = 0.05$). (*G*) Flow cytometric analysis of neonatal CD93^{+} immature splenic B cells. A representative of 14-d-old mice. (*H*) Transitional B-1a cell frequencies (*Left*) and numbers (*Right*) from neonatal spleens as in *G*. Data are from at least three mice of each genotype and are presented as mean ± SEM. Cell frequency at 1 d ($^{*}P = 0.019$); cell numbers at 1 d ($^{*}P = 0.019$). (*I*) Flow cytometric mean PTIP-GFP expression intensities relative to WT controls on freshly isolated splenic transitional B cells at the indicated ages from at least three mice. Three-day CD5^{+} transitional vs. 5-wk T1 ($^{***}P = 0.0007$), 3-d T1 vs. 5-wk T1 ($^{****}P < 0.0001$). Statistics were performed by using a two-tailed unpaired *t* test with Welch's correction.

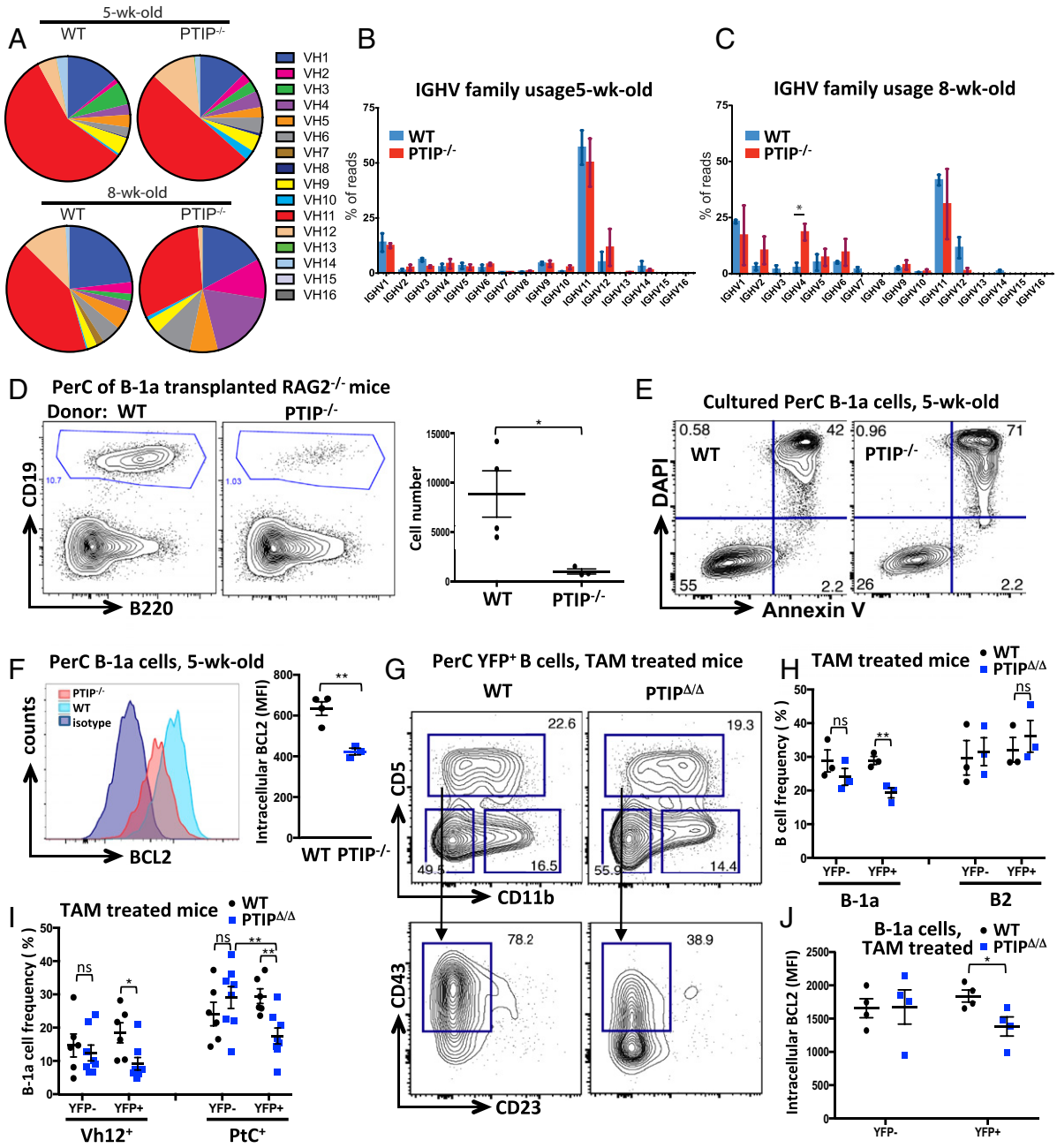

Fig. 4. PTIP-deficient B-1a cells are unable to maintain long-term survival of self-reactive clones. (*A*) Usage frequencies of the indicated BCR IgM heavy-chain V-segment families (IGHV) in the peritoneal B-1a population of 5- and 8-wk-old mice. Data are from at least three mice for each age and genotype and are presented as means. (*B* and *C*) V-family usage frequencies of the indicated IgM VH gene segments (IGHV) in sorted B-1a cells from (*B*) 5-wk-old and (*C*) 8-wk-old mice (*$P = 0.03$). Data are from at least three mice for each age and genotype and are presented as mean ± SEM. (*D*, *Left*) Flow cytometric analysis of B cells from peritoneal cavity of *RAG1*$^{-/-}$ 2 wk after transplantation of FACS sorted B-1a cells. A total of 40,000 WT or *PTIP*$^{-/-}$ FACS-sorted B-1a cells were injected i.p. into recipient *RAG1*$^{-/-}$ mice. (*D*, *Right*) B cell numbers from peritoneal cavities from at least three transplanted mice for each genotype. Data are presented as means (*$P = 0.04$). (*E*) Flow cytometric analysis of cultured B-1a cells from peritoneal cavity to assess survival after 48 h. Sorted B-1a cells were pooled from at least five mice of each genotype. (*F*) Flow cytometric analysis of BCL2 intracellular expression in B-1a cells from peritoneal cavities of 5-wk-old mice. (*Left*) Representative plot and (*Right*) mean expression intensities from at least three mice of each genotype (**$P = 0.004$). (*G*) Flow cytometric analysis of peritoneal cavity YFP$^+$ IgM$^+$CD19$^+$ B cells from mice 4 wk after TAM administration. (*Bottom*) Skewing of CD43 expression on CD5$^+$ B-1a cells in the mutant. Representative from multiple mice. Note the labeling of the *PTIP*$^{\Delta/\Delta}$ genotype, abbreviated from *Cre-ERT2*$^+$*Rosa26*$^{YFP/YFP}$*PTIP*^{floxIflox}, in which YFP is expressed (as a marker of Cre recombinase expression) upon TAM administration to the mice. WT mice have genotype *Cre-ERT2*$^+$*Rosa26*$^{YFP/YFP}$*PTIP*$^{+/+}$ and were administered TAM in parallel (statistics are shown in Fig. S4). (*H*) B cell frequencies within the YFP gate from peritoneal cavities of three mice of each genotype 1 wk after TAM administration. Data are presented as mean ± SEM. YFP$^+$ B-1a, *PTIP*$^{\Delta/\Delta}$ vs. WT [**$P = 0.008$; for other comparisons, $P > 0.05$, not significant (ns)]. (*I*) B-1a cell frequencies within the YFP gate displaying reactivity to Vh12 (*Left*) or PtC liposomes (*Right*) from peritoneal cavities from at least six mice of each genotype 4 wk after TAM administration. Data are presented as mean ± SEM. YFP$^+$ Vh12$^+$, *PTIP*$^{\Delta/\Delta}$ vs. WT (*$P = 0.029$); YFP$^-$ Vh12$^+$, *PTIP*$^{\Delta/\Delta}$ vs. WT [$P = 0.6$, not significant (ns)]. YFP$^+$ PtC liposome$^+$, *PTIP*$^{\Delta/\Delta}$ vs. WT (**$P = 0.003$); *PTIP*$^{\Delta/\Delta}$ PtC liposome$^+$, YFP$^+$ vs. YFP$^-$ (**$P = 0.01$); YFP$^-$ PtC liposome$^+$, *PTIP*$^{\Delta/\Delta}$ vs. WT [$P =$ 0.3, not significant (ns)]. (*J*) Mean BCL2 intracellular expression intensities in peritoneal cavity B-1a cells from four mice of each genotype 4 wk after TAM administration. YFP$^+$, *PTIP*$^{\Delta/\Delta}$ vs. WT (*$P = 0.04$). Data representative of two independent experiments. Statistics were obtained by using a two-tailed unpaired *t* test with Welch's correction.

B-1a cells from 5-wk-old mice were found to have a reduced frequency of live Annexin V$^-$DAPI$^-$ cells after 48 h (Fig. 4*E*). Consistent with these results, we measured the expression of the antiapoptotic BCL2 gene and found it to be significantly reduced at the mRNA and protein levels in *PTIP*$^{-/-}$ B-1a cells compared with controls (Fig. 4*F* and Fig. S4*A*). We conclude that PTIP promotes B-1a cell survival and is associated with increased BCL2 expression.

To formally rule out any developmental influence on B-1a cell survival, we crossed *PTIP*$^{flox/flox}$ mice with a mouse strain expressing tamoxifen (TAM)-inducible Cre-ERT2 to assess the effects of TAM-induced deletion of PTIP expression. In adult mice, bone marrow-dependent influx into the B-1a compartment is low; therefore, any observed phenotypes in the immediate weeks following TAM treatment of adult mice can be attributed to changes in the functionality of mature B-1a cells rather than developmental consequences. To visualize the frequency of Cre recombinase-expressing cells in these mice, we crossed in the Rosa26-stop-YFP Cre-reporter allele to generate *Cre-ERT2*$^+$*Rosa26*$^{YFP/YFP}$*PTIP*$^{flox/flox}$ (herein referred to as *PTIP*$^{\Delta/\Delta}$) and control mice (*Cre-ERT2*$^+$*Rosa26*$^{YFP/YFP}$*PTIP*$^{+/+}$, herein referred to as WT). Upon validating efficient Cre-mediated deletion (Fig. S4 *B*–*D*), we observed that several in vivo phenotypes of *PTIP*$^{-/-}$ mice were also recapitulated following inducible PTIP deletion. First, a significant decrease in the frequency of B-1a but not B-2 B cells could be observed among YFP$^+$ peritoneal cavity cells of *PTIP*$^{\Delta/\Delta}$ mice after TAM administration (Fig. 4 *G* and *H* and Fig. S4*E*). Second, within the B-1a cell gate, frequencies of VH12$^+$ and PtC liposome$^+$ cells were decreased in YFP$^+$ cells of *PTIP*$^{\Delta/\Delta}$ mice (Fig. 4*I* and Fig. S4*F*), consistent with PTIP being required for self-antigen driven peripheral maintenance (Fig. 4 *A*–*C*). Finally, YFP$^+$ B-1a cells from treated *PTIP*$^{\Delta/\Delta}$ mice displayed decreased BCL2 expression compared with controls (Fig. 4*J* and Fig. S4*G*). Taken together, these results formally establish a crucial role for PTIP in the survival of adult B-1a cells that is distinct from any developmental effects of PTIP deficiency.

PTIP Is Required for B Cell Activation via the NF-κB Pathway. To elucidate the molecular function of PTIP, we subjected sorted B-1a cells from 5-wk-old *PTIP*$^{-/-}$ and control animals to microarray-based global analyses of gene expression changes. In total, PTIP-deficient B-1a cells revealed 137 genes whose expression was down-regulated and 78 genes whose expression was up-regulated by at least twofold (Dataset S1). Interestingly, many differentially expressed genes were associated with signal transduction in the immune system, indicative of a role for PTIP in regulating signaling events (Fig. 5*A*). To further investigate this notion, we screened for the expression of a panel of proteins known to play a role in B-1a cell signaling by FACS. Although many of these did not change (CD19, BAFFR, and IL5RA; Fig. S5*A*), a few notable proteins were differentially expressed in the absence of PTIP. These include decreased Ceacam1/CD66a (Fig. 5*B*) and FcγRIIB (Fig. S5*A*), which were identified by the microarray, as well as increased CD72 (Fig. 5*C*) and CD22, and decreased CD43 and Siglec-G (Fig. S5*A*). Notably, Ceacam1 promotes signaling through the canonical NF-κB pathway (19), whereas CD72 can oppose it (20). Furthermore, the microarray identified an increase in the mRNA levels of *Anxa1*, encoding Annexin A1, a negative regulator of canonical NF-κB signaling (21, 22) (Dataset S1). Increased Annexin A1 was validated at the protein level by intracellular FACS in B-1a, B-1b, and B-2 B cells (Fig. 5*D*). These findings are intriguing in lieu of the crucial role of the NF-κB pathway in promoting B-1 and MZ B cell development as well as B cell survival through the regulation of Bcl2 family members (23, 24). To further investigate a potential role of PTIP in NF-κB signaling, we measured the expression of NF-κB proteins in freshly isolated *PTIP*$^{-/-}$ B-1a cells from 5-wk-old mice. These analyses revealed decreased intracellular levels of cREL (Fig. 5 *E* and *F*) along with NF-κB targets urokinase plasminogen activator (uPA) and IRF4 (Fig. S5*A*), suggesting that the absence of PTIP may perturb the classical NF-κB pathway and thereby lead to the observed impairments in the B-1 population.

The molecular program of steady-state B-1 cells often shares characteristics with that of their activated FO B-2 counterparts (2). Thus, we hypothesized that, even though PTIP only subtly reduces FO B-2 numbers at steady state (Fig. 2 *D* and *E*), it may regulate their function upon activation. Consistent with this notion, we found PTIP protein expression in mature splenic B cells cultured for 3 d to be increased 2.5-fold, 3.6-fold, or 5.2-fold upon anti-CD40, LPS, or BCR cross-linking, respectively, by using *PTIP*$^{gfp/gfp}$ mice (Fig. 5*G* and Fig. S5*B*). To directly assess the role of PTIP in BCR-induced FO B-2 B cell activation, we first measured cell proliferation by way of carboxyfluorescein *N*-hydroxysuccinimidyl ester (CFSE) dilution. Strikingly, proliferation of *PTIP*$^{-/-}$ splenic B cells was entirely abrogated in response to stimulation with anti-IgM antibody (Fig. 5*H* and Fig. S5*C*), with fewer cells undergoing active DNA replication as measured by EdU incorporation (Fig. S5*D*). An impairment in proliferation was also observed in *PTIP*$^{-/-}$ B cells in response to anti-CD40 (Fig. 5*H* and Fig. S5*C*). Interestingly, LPS and the TLR9 ligand CpG oligonucleotide stimulations induced extensive proliferation in WT and *PTIP*$^{-/-}$ B cells, although the fraction of B cells that underwent activation-induced proliferation was subtly decreased in the absence of PTIP (Fig. 5*H* and Fig. S5 *C* and *D*). Survival of *PTIP*$^{-/-}$ B cells was reduced by 2.4-fold upon stimulation with anti-IgM antibody but was less affected in response to other stimulations (Fig. S5*E*). Together, these data suggest that PTIP is required for specific aspects of B-2 cell activation downstream of antigen- and T:B interaction-induced activation rather than general cell cycle progression. Consistent with this notion, stimulated *PTIP*$^{-/-}$ B cells showed reduced cell surface expression of the CD86 activation marker in vitro and in vivo following anti-IgM stimulation and SRBC immunization, respectively (Fig. S6 *A* and *B*). These results indicate a crucial role for induced PTIP protein levels in propagating molecular events downstream of BCR ligation.

To identify signaling pathways that might be altered in PTIP-deficient FO B-2 B cells, we performed intracellular FACS analyses for phosphorylation events triggered by BCR cross-linking. We found no differences with respect to phospho-S6 (Fig. S6*C*), phospho-ERK (Fig. S6*D*), phospho-JNK (Fig. S6*E*), or phospho-SYK (Fig. S6*F*), consistent with normal membrane-proximal signaling and activation of the PI3K/AKT/mTOR and MAPK pathways. We did, however, detect significantly decreased protein expression of cREL (Fig. 5*I* and Fig. S6*G*) and the NF-κB target genes NFATc1, BCLXL, and BCL2 in *PTIP*$^{-/-}$ B cells (Fig. S6 *G* and *H*). These results constitute further evidence that the classical NF-κB pathway is impaired in the absence of PTIP. Consistent with these data, we observed elevated levels of IκBα in both freshly isolated and anti-IgM-stimulated FO B-2 B cells from *PTIP*$^{-/-}$ mice (Fig. S6*I*). The classical and the alternative NF-κB pathways are activated in B cells when stimulated with anti-CD40 antibody (25, 26). To determine whether PTIP also regulates the alternative NF-κB pathway, we interrogated the expression of RELB and its target gene PIM2 in anti-CD40 stimulated *PTIP*$^{-/-}$ and control B cells. Although we again observed decreased cREL expression, RELB and PIM2 were unchanged (Fig. 5*J* and Fig. S6*J*). Altogether, these results demonstrate a requirement for PTIP in promoting signaling via the classical NF-κB pathway in steady-state B-1a cells and FO B-2 B cells in response to BCR or CD40 engagement, providing an explanation for the apparent lack of postimmune antibody and GC responses upon TI and TD immunizations (Fig. 1).

Discussion

In this study, we use mouse genetics to establish a crucial role for PTIP in licensing the humoral arm of the adaptive immune system in vivo, through regulating key activation and signaling

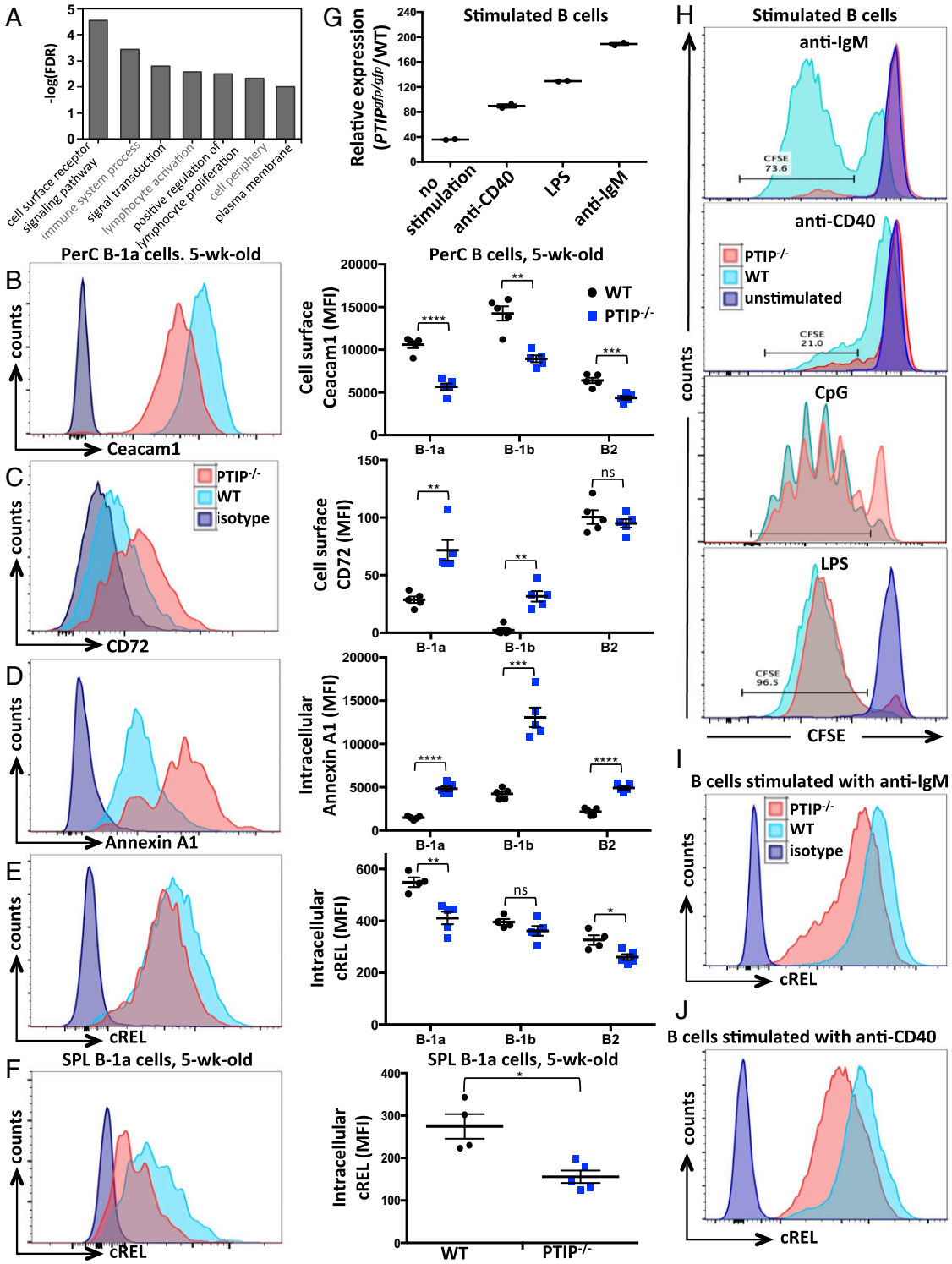

Fig. 5. PTIP is required for B cell activation via the NF-κB pathway. (*A*) Canonical pathways and biological processes overrepresented in the genes deregulated from microarray analysis of *PTIP*$^{-/-}$ relative to control-sorted B-1a cells from 5-wk-old mice. (*B–E*) Flow cytometric analysis of Ceacam1 (*B*) and CD72 (*C*) surface expression and Annexin A1 (*D*) and cREL (*E*) intracellular expression in B cells from peritoneal cavities of 5-wk-old mice. (*Left*) A representative plot from B-1a cells. (*Right*) Mean expression intensities in peritoneal cavity B cells from at least four mice of each genotype. (*B*) B-1a (****$P <$ 0.0001); B-1b (**$P = 0.002$); B-2 (***$P = 0.001$). (*C*) B-1a (**$P = 0.007$); B-1b (**$P = 0.002$); B-2 [$P = 0.47$, not significant (ns)]. (*D*) B-1a (****$P = 0.0001$); B-1b (***$P = 0.001$); and B-2 (****$P <$ 0.0001). (*E*) B-1a (**$P = 0.003$); B-1b [$P = 0.16$, not significant (ns)]; B-2 (*$P = 0.03$). (*F*) Flow cytometric analysis of cREL intracellular expression in B-1a cells from spleens of 5-wk-old mice. (*Left*) Representative plot. (*Right*) Mean expression intensities in splenic B cells from four mice of each genotype (*$P = 0.018$). Statistics were obtained by using a two-tailed unpaired *t* test with Welch's correction. (*G*) Flow cytometric mean PTIP-GFP expression intensities in splenic B cells relative to WT controls from two adult mice after 3 d of the indicated stimulation. (*H*) Flow cytometric analysis of CFSE-labeled splenic B cells with or without the indicated stimulation for 3 d. (*I*) Flow cytometric analysis of cREL intracellular expression in splenic B cells stimulated with anti-IgM for 18 h. (*J*) Flow cytometric analysis of cREL intracellular expression in splenic B cells stimulated with anti-CD40 for 24 h. (*H–J*) Representatives from multiple mice 7–8 wk of age, with statistics shown in Fig. S5.

events critical for multiple aspects of B cell development and function (Fig. 6). By using a PTIP-GFP knock-in mouse model, we demonstrate that cellular levels of PTIP protein correlate with BCR signaling strength, being elevated in steady-state innate-like B cell subsets and stimulated FO B cells. By using mice that lack PTIP in a B cell-specific manner, we show a partial block in B cell development at the pre-B cell stage, a severe impairment in neonatal B-1a cell maturation, and defective GC B cell differentiation. In addition, we find that sustained PTIP expression in adult mice is required to promote the long-term maintenance of bona fide self-reactive B-1a cells. Although the steady-state numbers of splenic B-2 cells are not markedly reduced in PTIP-deficient mice, these cells fail to undergo BCR or CD40 stimulation-induced proliferation, at least in part, because of a defect in the classical NF-κB pathway. These results significantly expand the list of PTIP-dependent B cell functions beyond promoting sterile transcription at the *Igh* locus and CSR (6, 8, 9) and indicate a key role for PTIP in activation-associated proliferation, survival, and differentiation triggered by antigen engagement and T:B interaction. Consequently, PTIP deficiency results in severe hypo-IgM, hypogammaglobulinemia, and profoundly blunted antibody responses to TD and TI antigen immunization, hallmarks of primary common variable immunodeficiency (CVID).

Although the precise molecular targets by which PTIP mediates its function in B cell signaling remain to be elucidated, we provide multiple lines of evidence in PTIP-deficient B-1a cells and activated B-2 B cells for deregulation of the classical NF-κB pathway. In addition to decreased cREL and increased IκBα at steady state and in response to anti-IgM, we find protein levels of a handful of NF-κB target genes to be decreased in PTIP-deficient B cells, including BCL2, BCLXL (27, 28), NFATc1 (29), uPA, IRF4 (30), and CD23 (31). These findings indicate a requirement for PTIP in the classical NF-κB pathway and are in line with (*i*) the established role of the NF-κB pathway in B-1 cell development (15, 24, 25, 32), (*ii*) evidence for a role of NF-κB downstream of pre-BCR signaling in small pre-B cells (28, 33–36), and (*iii*) FO B-2 cell functionality including activation-induced proliferation, survival, antibody production, GC differentiation, and CSR (24–26, 37). Although the role of NF-κB signaling in the development of FO B cells may primarily be to promote BCL2 or BCLXL expression for antiapoptotic effects (27, 28, 34), evidence suggests that BCL2-independent functions of NF-κB play a major role in B-1, MZ, and GC B cells and hint at prominent roles during activation-associated differentiation (24, 27, 37). Considering that the cREL NF-κB protein plays an important role in antigen-mediated BCR activation (38) and that sustained cREL activation in response to BCR signaling requires de novo cREL transcription (39), we speculate that PTIP may function in the activation and/or expression of this protein. Several other PTIP-regulated genes have also previously been shown to influence the NF-κB pathway including CD72 (20, 40), Ceacam1 (19), and Annexin A1 (21, 22). Future studies aimed at determining the contribution of each of these signaling components to the various junctures of PTIP involvement in B cell biology (Fig. 6) will be needed to map the PTIP-dependent genetic program establishing humoral immunity.

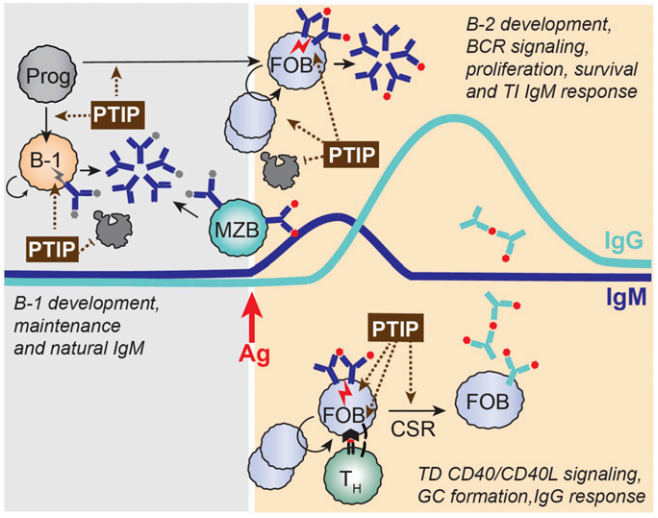

Fig. 6. Model showing multiple points of PTIP involvement in B cell activation-associated proliferation/differentiation for licensing humoral immunity. PTIP regulates multiple aspects of B cell development and function including (*i*) the development of B-1 B cells in neonatal life and their self-renewal/survival in adult life, contributing to natural IgM levels in serum before antigen stimulation; (*ii*) efficient differentiation of small pre-B cells in response to pre-BCR signaling during B cell development; (*iii*) facilitating signal transduction in response to BCR engagement to promote B cell activation and proliferation/survival, contributing to TI production of antigen-specific IgM during the initial phase of the antibody response; (*iv*) facilitating signal transduction in response to CD40/CD40L engagement to promote B cell activation and proliferation upon cognate T cell-B cell interaction including GC B cell differentiation; and (*v*) activating sterile transcription at "switch regions" within the *Igh* locus to promote IgG class-switching. Ag, antigen; Prog, progenitor; T_H, helper T cell. Gray dots signify self-antigens; red dots signify foreign antigens.

The striking lack of steady-state levels of serum IgM in PTIP-deficient mice despite normal numbers of overall splenic B cells correlates with the combined loss of B-1 and MZ B cells. These innate-like B cell subsets act in concert to mediate the majority of TI antibody production (2–4), and their development differs from FO B-2 cells in their increased dependency on BCR signaling. For example, B-1a and MZ B cells are positively selected on self-antigen during maturation and their unique clonal representation depends on continued self-antigen exposure (12, 13, 17). Indeed, numerous mouse models deficient in B-1 cells show concomitant defects in MZ B cells (3, 25), including those harboring perturbations in BCR signaling and the NF-κB pathway. We speculate that the B-1 and MZ B cell defects associated with PTIP deficiency stem from a common impairment in signaling and manifest together as a general reduction in natural and postimmune IgM levels. Furthermore, the aforementioned characteristics of innate-like B cells along with the observed higher PTIP protein levels in B-1 and MZ B cells compared with FO B cells are consistent with PTIP protein expression being positively regulated by BCR signaling. Similarly, the elevated expression of and reliance on PTIP protein during neonatal B lymphopoiesis hint toward elevated BCR signaling early in life.

PTIP is a multifunctional chromatin regulator known to dynamically contribute to several multimeric protein complexes to regulate transcription and DNA repair in response to changes in cellular demand (5). A common denominator for our observed PTIP functions in humoral immunity, including the previously described regulation of sterile transcription at the *Igh* locus (6, 8), is that they operate independently from its interaction with the 53BP1 DNA repair protein. Consistent with this, perturbations of other DNA damage response factors do not impact steady-state or postimmune IgM responses. Moreover, B cells lacking PTIP do not have an inherent defect in cell cycle progression. Thus, we speculate that PTIP-dependent transcriptional regulation rather than its involvement in DNA repair/replication is responsible for the observed effects on humoral immunity. Although MLL4 complexes containing PTIP have been shown to regulate B cell gene expression, phenotypic differences between PTIP- and MLL4-deficient mice (6, 41, 42) point toward an MLL4-independent role for PTIP in humoral immunity.

Although much remains to be understood about how PTIP is regulated by, and in turn regulates, BCR and T:B interaction-triggered molecular events, a model is emerging in which PTIP fundamentally controls humoral immunity at multiple junctures of B cell development and differentiation

(Fig. 6). Our results place PTIP in a molecular node required for B cell activation important for humoral immune responses in health and disease. CVID is the most prevalent primary antibody deficiency; with a highly heterogeneous disease origin, the genetic abnormality remains unknown in a majority of patients (43). Further work investigating the mechanism of PTIP function in this context and how it controls the NF-κB pathway may generate valuable new insight.

Materials and Methods

Bone marrow and spleens were subjected to RBC lysis. Antibodies are detailed in Table S1. FACS experiments on freshly isolated cells used a DAPI negative live lymphocyte gate. Intracellular staining experiments used the Zombie Aqua fixable viability kit (BioLegend). Cells were acquired on BD LSRFortessa and sorted on a BD FACSAria III Cell Sorter. All other methods are described in *SI Materials and Methods*.

ACKNOWLEDGMENTS. We thank G. Cruz for FACS sorting, O. Østrup for microarray analysis, K. Rajewsky for Vh12 antibody, University of Copenhagen Department of Experimental Medicine animal caretakers, and A. Mund for discussions. This work was supported by Independent Research Fund Denmark with a Sapere Aude Starting Grant (to J.A.D.) and postdoctoral fellowship (to L.M.S.); the Danish Cancer Society (to J.A.D.); Novo Nordisk Foundation Grant NNF14CC0001 (to J.A.D.); and grants from the Swedish Cancer Foundation (to J.Y.), Swedish Research Council (to J.Y.), European Research Council (to J.Y.), StemTherapy (to J.Y.), Knut and Alice Wallenberg Foundation (to J.Y.), Swedish Cancer Foundation (to E.J.G.), and Wenner–Gren Foundations (to S.V.).

1. Baumgarth N, et al. (1999) Innate and acquired humoral immunities to influenza virus are mediated by distinct arms of the immune system. *Proc Natl Acad Sci USA* 96: 2250–2255.
2. Baumgarth N (2016) B-1 cell heterogeneity and the regulation of natural and antigen-induced IgM production. *Front Immunol* 7:324.
3. Martin F, Oliver AM, Kearney JF (2001) Marginal zone and B1 B cells unite in the early response against T-independent blood-borne particulate antigens. *Immunity* 14: 617–629.
4. Haas KM, Poe JC, Steeber DA, Tedder TF (2005) B-1a and B-1b cells exhibit distinct developmental requirements and have unique functional roles in innate and adaptive immunity to S. pneumoniae. *Immunity* 23:7–18.
5. Daniel JA, Nussenzweig A (2013) The AID-induced DNA damage response in chromatin. *Mol Cell* 50:309–321.
6. Starnes LM, et al. (2016) A PTIP-PA1 subcomplex promotes transcription for IgH class switching independently from the associated MLL3/MLL4 methyltransferase complex. *Genes Dev* 30:149–163.
7. Callen E, et al. (2013) 53BP1 mediates productive and mutagenic DNA repair through distinct phosphoprotein interactions. *Cell* 153:1266–1280.
8. Daniel JA, et al. (2010) PTIP promotes chromatin changes critical for immunoglobulin class switch recombination. *Science* 329:917–923.
9. Schwab KR, Patel SR, Dressler GR (2011) Role of PTIP in class switch recombination and long-range chromatin interactions at the immunoglobulin heavy chain locus. *Mol Cell Biol* 31:1503–1511.
10. Manis JP, et al. (2004) 53BP1 links DNA damage-response pathways to immunoglobulin heavy chain class-switch recombination. *Nat Immunol* 5:481–487.
11. Ward IM, et al. (2004) 53BP1 is required for class switch recombination. *J Cell Biol* 165: 459–464.
12. Hayakawa K, et al. (1999) Positive selection of natural autoreactive B cells. *Science* 285:113–116.
13. Wen L, et al. (2005) Evidence of marginal-zone B cell-positive selection in spleen. *Immunity* 23:297–308.
14. Montecino-Rodriguez E, Dorshkind K (2012) B-1 B cell development in the fetus and adult. *Immunity* 36:13–21.
15. Montecino-Rodriguez E, Dorshkind K (2011) Formation of B-1 B cells from neonatal B-1 transitional cells exhibits NF-κB redundancy. *J Immunol* 187:5712–5719.
16. Pedersen GK, et al. (2014) B-1a transitional cells are phenotypically distinct and are lacking in mice deficient in IκBNS. *Proc Natl Acad Sci USA* 111:E4119–E4126.
17. Yang Y, et al. (2015) Distinct mechanisms define murine B cell lineage immunoglobulin heavy chain (IgH) repertoires. *eLife* 4:e09083.
18. Mercolino TJ, Arnold LW, Hawkins LA, Haughton G (1988) Normal mouse peritoneum contains a large population of Ly-1+ (CD5) B cells that recognize phosphatidyl choline. Relationship to cells that secrete hemolytic antibody specific for autologous erythrocytes. *J Exp Med* 168:687–698.
19. Khairnar V, et al. (2015) CEACAM1 induces B-cell survival and is essential for protective antiviral antibody production. *Nat Commun* 6:6217.
20. Li DH, et al. (2006) CD72 down-modulates BCR-induced signal transduction and diminishes survival in primary mature B lymphocytes. *J Immunol* 176:5321–5328.
21. Zhang Z, Huang L, Zhao W, Rigas B (2010) Annexin 1 induced by anti-inflammatory drugs binds to NF-kappaB and inhibits its activation: Anticancer effects in vitro and in vivo. *Cancer Res* 70:2379–2388.
22. Bist P, et al. (2011) Annexin-1 interacts with NEMO and RIP1 to constitutively activate IKK complex and NF-κB: Implication in breast cancer metastasis. *Oncogene* 30: 3174–3185.
23. Pedersen GK, Ádori M, Karlsson Hedestam GB (2015) NF-κB signaling in B-1 cell development. *Ann N Y Acad Sci* 1362:39–47.
24. Derudder E, et al. (2016) Canonical NF-κB signaling is uniquely required for the long-term persistence of functional mature B cells. *Proc Natl Acad Sci USA* 113:5065–5070.
25. Sasaki Y, Iwai K (2016) Roles of the NF-κB pathway in B-lymphocyte biology. *Curr Top Microbiol Immunol* 393:177–209.
26. Gerondakis S, Siebenlist U (2010) Roles of the NF-kappaB pathway in lymphocyte development and function. *Cold Spring Harb Perspect Biol* 2:a000182.
27. Grossmann M, et al. (2000) The anti-apoptotic activities of Rel and RelA required during B-cell maturation involve the regulation of Bcl-2 expression. *EMBO J* 19: 6351–6360.
28. Derudder E, et al. (2009) Development of immunoglobulin lambda-chain-positive B cells, but not editing of immunoglobulin kappa-chain, depends on NF-kappaB signals. *Nat Immunol* 10:647–654.
29. Berland R, Wortis HH (2003) Normal B-1a cell development requires B cell-intrinsic NFATc1 activity. *Proc Natl Acad Sci USA* 100:13459–13464.
30. Grumont RJ, Gerondakis S (2000) Rel induces interferon regulatory factor 4 (IRF-4) expression in lymphocytes: Modulation of interferon-regulated gene expression by rel/nuclear factor kappaB. *J Exp Med* 191:1281–1292.
31. Lu KT, Sinquett FL, Dryer RL, Song C, Covey LR (2006) c-Rel plays a key role in deficient activation of B cells from a non-X-linked hyper-IgM patient. *Blood* 108:3769–3776.
32. Pohl T, et al. (2002) The combined absence of NF-kappa B1 and c-Rel reveals that overlapping roles for these transcription factors in the B cell lineage are restricted to the activation and function of mature cells. *Proc Natl Acad Sci USA* 99:4514–4519.
33. Jimi E, et al. (2005) Activation of NF-kappaB promotes the transition of large, CD43+ pre-B cells to small, CD43- pre-B cells. *Int Immunol* 17:815–825.
34. Feng B, Cheng S, Pear WS, Liou H-C (2004) NF-kB inhibitor blocks B cell development at two checkpoints. *Med Immunol* 3:1.
35. Claudio E, Saret S, Wang H, Siebenlist U (2009) Cell-autonomous role for NF-kappa B in immature bone marrow B cells. *J Immunol* 182:3406–3413.
36. Scherer DC, et al. (1996) Corepression of RelA and c-rel inhibits immunoglobulin kappa gene transcription and rearrangement in precursor B lymphocytes. *Immunity* 5: 563–574.
37. Heise N, et al. (2014) Germinal center B cell maintenance and differentiation are controlled by distinct NF-κB transcription factor subunits. *J Exp Med* 211:2103–2118.
38. Grumont RJ, et al. (1998) B lymphocytes differentially use the Rel and nuclear factor kappaB1 (NF-kappaB1) transcription factors to regulate cell cycle progression and apoptosis in quiescent and mitogen-activated cells. *J Exp Med* 187:663–674.
39. Castro I, et al. (2009) B cell receptor-mediated sustained c-Rel activation facilitates late transitional B cell survival through control of B cell activating factor receptor and NF-kappaB2. *J Immunol* 182:7729–7737.
40. Pan C, Baumgarth N, Parnes JR (1999) CD72-deficient mice reveal nonredundant roles of CD72 in B cell development and activation. *Immunity* 11:495–506.
41. Ortega-Molina A, et al. (2015) The histone lysine methyltransferase KMT2D sustains a gene expression program that represses B cell lymphoma development. *Nat Med* 21: 1199–1208.
42. Zhang J, et al. (2015) Disruption of KMT2D perturbs germinal center B cell development and promotes lymphomagenesis. *Nat Med* 21:1190–1198.
43. Bonilla FA, Geha RS (2009) Common variable immunodeficiency. *Pediatr Res* 65: 13R–19R.
44. Kim D, Wang M, Cai Q, Brooks H, Dressler GR (2007) Pax transactivation-domain interacting protein is required for urine concentration and osmotolerance in collecting duct epithelia. *J Am Soc Nephrol* 18:1458–1465.
45. Zhang J, Kobert K, Flouri T, Stamatakis A (2014) PEAR: A fast and accurate Illumina Paired-End reAd mergeR. *Bioinformatics* 30:614–620.
46. Alamyar E, Duroux P, Lefranc M-P, Giudicelli V (2012) IMGT(®) tools for the nucleotide analysis of immunoglobulin (IG) and T cell receptor (TR) V-(D)-J repertoires, polymorphisms, and IG mutations: IMGT/V-QUEST and IMGT/HighV-QUEST for NGS. *Methods Mol Biol* 882:569–604.